BIOCHEMISTRY

 Volume 45, Number 3 January 24, 2006

Accelerated Publications

Chaperone Holdase Activity of Human Papillomavirus E7 Oncoprotein†

Leonardo G. Alonso, Clara Smal, Maria M. Garcia-Alai, Lucia Chemes, Marcelo Salame, and Gonzalo de Prat-Gay*

Instituto Leloir and CONICET, Patricias Argentinas 435, 1405 Buenos Aires, Argentina

Received November 3, 2005; Revised Manuscript Received December 1, 2005

ABSTRACT: E7 oncoprotein is the major transforming activity in human papillomavirus and shares sequence and functional properties with adenovirus E1A and SV40 T-antigen, in particular by targeting the pRb tumor suppressor. HPV 16 E7 forms spherical oligomers that display chaperone activity in thermal denaturation and chemical refolding assays of two model polypeptide substrates, citrate synthase and luciferase, and it does so at substoichiometric concentrations. We show that the E7 chaperone can stably bind model polypeptides and hold them in a state with significant tertiary structure, but does not bind the fully native proteins. The E7 oligomers bind native in vitro translated pRb without the requirement of it being unfolded, since the N-terminal domain of E7 containing the LXCXE binding motif is exposed. The N-terminal domain of E7 can interfere with pRb binding but not with the chaperone activity, which requires the C-terminal domain, as in most reported E7 activities. The ability to bind up to ~72 molecules of pRb by the oligomeric E7 form could be important either for sequestering pRb from Rb−E2F complexes or for targeting it for proteasome degradation. Thus, both the dimeric and oligomeric chaperone forms of E7 can bind Rb and various potential targets. We do not know at present if the chaperone activity of E7 plays an essential role in the viral life cycle; however, a chaperone activity may explain the large number of cellular targets reported for this oncoprotein.

Papillomaviruses, in particular, certain human-infecting strains, are directly linked to the development of cervical cancer, a major cause of women's death worldwide. They are small double-stranded DNA viruses, with a genome of 8 kb expressing eight to nine proteins. These viruses cannot replicate their DNA autonomously and are very effective in taking advantage of the cellular machinery to complete a productive life cycle. This phenomenon is common to other DNA tumor viruses such as adenovirus and SV40, and the way to achieve this is by hijacking the DNA replication machinery of the infected cells, forcing them to enter S phase, where they actively replicate their viral episomal genomes. In addition, these viruses and their oncoproteins have been essential in understanding the molecules and mechanisms involved in cell cycle progression and carcinogenesis (*1*, *2*).

Two early proteins are mainly responsible for the human papillomavirus (HPV[1])-mediated malignant cell progression, leading ultimately to an invasive carcinoma. These are the E6 and E7 proteins, which cooperate for the transformation of rodent cell lines, established as a reference assay (*3*). Although E6 contributes to cellular transformation, it does not have a major transformation activity by itself. The major

† This work was supported by ICGEB (CRP ARG0102) and ANPCyT (PICT 01-10944). G.d.P.-G. is a Career Investigator from CONICET. L.G.A. holds a Ph.D. studentship from CONICET, and M.G.A. and C.S. hold Ph.D. studentships from the University of Buenos Aires.

* To whom correspondence should be addressed. Fax: 054-11-52387501. Phone: 054-11-52387500. E-mail: gpratgay@leloir.org.ar.

10.1021/bi0522549 CCC: $33.50
Published on Web 12/24/2005

transforming activity has been mapped to E7 from mutational analysis (*4*, *5*). Both oncoproteins are known to exert pleiotropic effects on infected cells, with an increasing number of targets being described (*6*, *7*). The main targets of E6 and E7 are the tumor suppressors p53 and retinoblastoma protein (pRb), respectively (*8*). HPV E7 proteins are fairly unstable in the cell, and are rapidly degraded by the ubiquitin proteasome system (*9*, *10*). E7 shares regions of homology with the SV40 T-antigen and adenovirus E1A proteins, and was shown to share biological properties as well (*4*). All three oncoproteins bind to pRb and the pocket family members through the LXCXE sequence motif.

A main property of these oncoproteins is their ability to sequester the hypophosphorylated form of the pRb tumor suppressor and other so-called pocket proteins and target them for degradation. In the G0−G1 phase, pRb is bound to members of the family of E2F general transcriptional activator and its phosphorylation causes the release of E2F, with the consequent induction of the cellular DNA synthesis machinery (*11*). In addition, high-risk HPV E7 binds to pRb and promotes its degradation through the proteasome system (*12*−*14*), thus deregulating the cell cycle, and also releasing active E2F (*14*). The correlation between high-level expression of E7 and reduced pRb levels was recently confirmed in cervical biopsies (*15*). Thus, the transformation activity of this oncoprotein correlates with its ability to promote pRb degradation (*12*). E7 forms from high-risk HPV-16 and -18 strains bind pRb tighter and are phosphorylated to a larger extent by CKII than the low-risk (HPV-11 and -6) counterparts, and this difference in affinity maps to the pRb binding site (*16*).

The E7 proteins are small (~100 amino acids) acidic proteins that bind zinc through their C-terminal domain, which was proposed to be involved in dimerization (*17*). There is neither structural information nor enzymatic activity reported for E7 protein, and its biochemistry is most intriguing. The only known biochemical activity is the binding of numerous cellular targets (*6*, *7*). We started a biophysical characterization of HPV-16 E7, puzzled by how such a small protein could display such a wide range of cellular targets. Chemically pure HPV-16 E7 expressed in *Escherichia coli* was conformationally heterogeneous in gel filtration chromatography, where the major species corresponds to a dimer with a molecular mass of 22 kDa. Although E7 exhibits properties that resemble those of natively unfolded polypeptides, its far-UV circular dichroism spectrum, cooperative unfolding, and exposure of 8-anilino-1-naphthalenesulfonate (ANS) binding sites support a folded albeit extended conformation (*18*). We recently reported that treatment with a chelating agent produces a protein that readily assembles into homogeneous spherical oligomeric particles (E7SOs) with a molecular mass of 790 kDa and a diameter of ~50 nm (*19*).

[1] Abbreviations: HPV, human papillomavirus; BPV, bovine papillomavirus; MBP, maltose binding protein; DTT, dithiothreitol; EDTA, ethylenediaminetetraacetic acid; Tris, tris(hydroxymethyl)aminomethane; BSA, bovine serum albumin; Gdm·Cl, guanidine hydrochloride; TCA, trichloroacetic acid; EGTA, ethylene glycol bis(β-aminoethyl ether)-*N*,*N*,*N*′,*N*′-tetraacetic acid; ANS, 8-anilino-1-naphthalenesulfonate; PMSF, phenylmethanesulfonyl fluoride; pRb, retinoblastoma protein; $E7_2$, E7 dimer; E7SOs, E7 high-molecular mass soluble oligomer.

Several lines of evidence led us to investigate the possibility that HPV E7 is a protein chaperone. In this work, we show that HPV-16 E7 displays ATP-independent chaperone holdase activity on two model chaperone substrate proteins: pig heart citrate synthase and luciferase. The substrates retain a significant degree of structure when bound to the E7SOs, and they do so substoichiometrically. The chaperone activity is the first biochemical activity described for an E7 protein and explains its wide target specificity, which appears to be separable from specific pRb binding.

MATERIALS AND METHODS

Protein Expression and Purification. Recombinant E7 HPV-16 protein was expressed and purified as previously described (*18*). MBP−E7 fusion protein was expressed and purified as described previously (*19*) except that the fraction that eluted from the amylose affinity column was subjected to a hydroxyapatite column to remove maltose from MBP protein, allowing rebinding to amylose in pull-down experiments. MBP−E7SOs fusion proteins were obtained as described for the nonfusion E7 protein (*19*). Briefly, the purified MBP−E7 dimer was incubated for 24 h in 10 mM sodium phosphate buffer (pH 7.0), 1.0 mM DTT, and 1.0 mM EDTA and dialyzed against the same buffer without EDTA. Pig heart citrate synthase was purchased from Sigma-Aldrich, and dissolved to 30 μM in 30 mM Tris (pH 8.0). D-Luciferin and firefly luciferase were from Apollo Scientific, and luciferase was stored in 30 mM Tris (pH 8). All protein concentrations refer to monomers.

Chaperone Activity. Pig heart CS or firefly luciferase (150 nM final concentration) was added to a 45 °C preheated solution containing varying amounts of $E7_2$, E7SOs, or BSA (protein control) in 25 mM sodium phosphate buffer (pH 7.0) and 1.0 mM DTT. Aggregation was followed by monitoring light scattering at 360 nm either in a spectrophotometer or in a fluorescence spectrophotometer with the excitation and emission wavelengths at 360 nm in a thermostated cuvette holder.

A titration experiment to determine the binding stoichiometry of the E7SOs−CS complex was performed by incubating a fixed CS concentration (0.15 μM) with increasing ratios of E7SOs, at 45 °C for 30 min, centrifuged for 30 min at 3500 rpm, and the soluble fraction was analyzed by 10% SDS−PAGE.

Chemically denatured CS was prepared as described previously (*26*). Briefly, an aliquot of CS (20 μM final concentration) was dissolved in 20 mM Tris buffer (pH 8.0), 6.0 M Gdm·Cl, and 5.0 mM DTT and incubated for 4 h. For light scattering measurements, chemically denatured CS was diluted to 150 nM in 25 mM sodium phosphate buffer (pH 7.0) and 1.0 mM DTT containing varying amounts of $E7_2$, E7SOs, or BSA at 25 °C under continuous stirring.

Size Exclusion Chromatography. Protein complexes were obtained by incubating 1.5 μM CS and 9.0 μM $E7_2$ or E7SOs in 250 μL of 25 mM sodium phosphate buffer (pH 7.0) at 45 or 25 °C for 30 min. Samples were centrifuged at room temperature for 10 min at 13 000 rpm and then analyzed by SEC using a BioSil 400 column (Bio-Rad). Running buffer consisted of 150 mM sodium phosphate (pH 7.0) and 1.0 mM DTT at a flow rate of 1 mL/min. Each peak was collected, precipitated with 10% (v/v) TCA, and analyzed

by 15% SDS−PAGE. MBP−E7SOs fusion proteins recovered from the amylose binding experiment were loaded onto a BioSil 200 SEC column equilibrated with 150 mM sodium phosphate (pH 7.0).

Luciferase Activity. Luciferase at 1.0 and 6.0 μM $E7_2$ or E7SOs was incubated for 30 min at the indicated temperature in 25 mM sodium phosphate buffer (pH 7.0) and 0.5 mg/mL BSA. Samples were cooled, diluted to a final luciferase concentration of 150 nM, and centrifuged for 20 min at 13 000 rpm. Luciferase activity present in 2 μL aliquots was determined by dilution into 50 μL of assay buffer containing 25 mM Tricine (pH 7.8), 8.0 mM SO_4Mg, 2.0 mM EGTA, 33 mM DTT, 0.5 mM ATP, 235 μM D-luciferin, and 120 μM coenzyme A.

Fluorescence Spectroscopy. Tryptophan emission spectra were recorded on an Aminco-Bowman spectrofluorimeter with an excitation wavelength of 290 nm at 25 °C. Samples were prepared by incubating 0.5 μM CS or luciferase with a 9-fold molar excess (considering monomeric concentration) of $E7_2$ or E7SOs at the stated temperature for 25 min, in 25 mM sodium phosphate buffer (pH 7.0), and centrifuged for 20 min at 13 000 rpm prior to being measured. Fluorescence emission spectra for ANS binding of the complexes were recorded after addition of 20 μM ANS (final concentration) to each sample, incubation for 2 h at 25 °C, and measurement with an excitation wavelength of 370 nm, with a 4 nm bandpass. An average of three spectra were processed.

Acrylamide quenching experiments were performed by titrating samples prepared as described above except that 1.0 μM CS was used with a freshly prepared 4.0 M acrylamide solution. Each point was measured with excitation and emission wavelengths of 295 and 330 nm, respectively, and corrected for dilution and blanks. Data were analyzed using the Stern−Volmer equation (*50*):

$$F_0/F = 1 + K_q[Q]$$

where F_0 is the fluorescence in the absence and F in the presence of quencher, K_q is the apparent quenching constant, and [Q] is the quencher concentration.

Amylose Binding. Two hundred microliters of MBP−E7SOs fusion protein at 0.5 mg/mL in 30 mM Tris (pH 7.5) was incubated with 150 μL of amylose beads (New England Biolabs) for 1 h at room temperature and centrifuged for 2 min at 3500 rpm, and the supernatant was discarded. The resin was then washed two times with 1 mL of 30 mM Tris (pH 7.5) and divided into 50 μL aliquots for each treatment. One aliquot was treated with 200 μL of buffer containing 15 mM maltose to elute the bound protein. Samples were resolved via 12.5% SDS−PAGE.

Rb−E7 Interaction. Full-length pRb105 and pocket domain p50 (amino acids 372−787) of pRb were cloned into the pRSet A vector (Invitrogen**)** translated in the presence of ^{35}S. Methionine using Promega's TNT rabbit reticulocyte lysate transcription and translation system according to the manufacturer's protocol to produce radiolabeled pRb. The binding reaction that includes 1 μL of pRb translated mix, 3 μg of E7 proteins, and 100 μM E7(1−40) when stated was carried out in 1 mL of binding buffer [25 mM HEPES (pH 7.5), 1 mM DTT, 0.5 mM PMSF, 0.1% Nonidet NP-40, 1 mg/mL BSA, and 0.125 M NaCl] for 30 min at 4 °C. Four microliters of anti-E7 IgG monoclonal antibody was added to the reaction mixture and the mixture incubated for 40 min at 4 °C with shaking prior to addition of 30 μL of a 50% (v/v) suspension of protein G−Sepharose beads (Amersham-Pharmacia) to immunoprecipitate the complex. Beads were washed three times with binding buffer and electrophoresed via 12.5% SDS−PAGE. ^{35}S-labeled pRb protein was visualized in a Storm 840 phosphorimager (Molecular Dynamics).

RESULTS

E7SOs Display Chaperone Activity at Substoichiometrical Concentrations. The precise molecular mechanism through which E7 performs its biological function remains elusive so far, but from a biochemical point of view, some properties arise as important hallmarks of this small polypeptide. First, it can bind a wide range of cellular protein targets despite its small size. Second, E7 produces various, sometimes opposing effects on its targets. Finally, the fast turnover and therefore low steady state concentration of this protein in naturally infected cells exclude the possibility that its functions are performed stoichiometrically (*20*).

The HSP family of proteins is a divergent growing group of folding accessory proteins present in almost all organisms investigated so far [α crystallin (*21*), HSP 16.5, HSP25 (*22*)] which share the property of preventing thermal or chemical aggregation and/or denaturation of substrate cellular proteins. These proteins form high-molecular mass soluble oligomers enriched in β-sheet secondary structure (*23*, *24*) that exhibit stronger ANS binding and lack any ATP requirement for their chaperone activity. Thus, HPV-16 E7 (i) has a wide target specificity that cannot be assigned to different domains due to its small size, (ii) is present in small amounts in the cell, suggesting substoichiometrical activity (in particular linked to part i), and (iii) forms large soluble oligomers, E7SOs, with stronger ANS binding and repetitive β-sheet content, and (iv) circumstantial evidence suggests that E7 proteins may utilize chaperone pathways to modulate pRb and related proteins (*25*). All this evidence prompted us to investigate a possible chaperone activity of E7.

To test for chaperone activity in E7, we carried out thermal and chemical denaturation experiments on two model substrate proteins, the dimeric citrate synthase (CS, 49 kDa) and the monomeric luciferase (Luc, 61 kDa), in the presence of E7SOs. Incubation of CS at 43 °C leads to the slow aggregation of the protein in the absence of additives, which is the basis for established chaperone activity assays [Figure 1, top panel (*26*)]. The addition of dimeric E7 ($E7_2$) at an up to 6-fold molar excess in monomer concentration, prior to heat treatment, does not prevent the temperature-mediated denaturation and aggregation of CS (Figure 1A). Under identical conditions, the addition of E7SOs to the mixture completely prevented aggregation of CS at an E7SO:CS ratio of 2:1 to 3:1 based on monomer concentration (Figure 1B). However, the molecular mass of the oligomers is 790 kDa, and on the basis of a molecular mass of 11 kDa for the E7 monomer, we can assume approximately 72 monomers per oligomer. Thus, the actual molar concentration of E7SOs is at least 72 times lower, so the molar concentration of E7SOs that completely suppresses aggregation is at least less than 100-fold lower than that of the substrate protein (Figure 1B, inset). Similarly, E7SOs readily prevent thermal aggregation of luciferase, whereas $E7_2$ or BSA does not (Figure 1C,D).

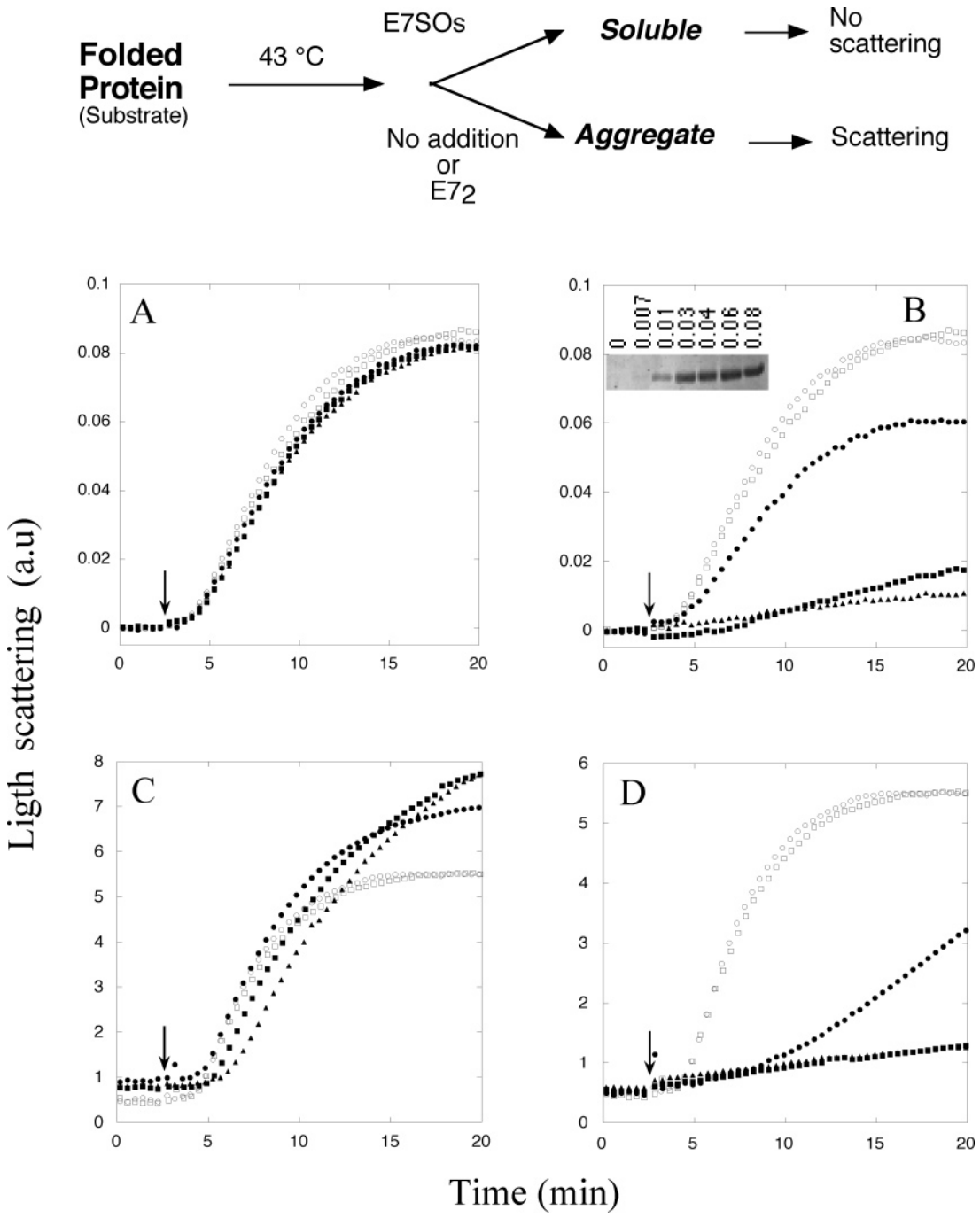

FIGURE 1: Chaperone activity of E7SOs on CS and firefly luciferase. The top panel is a schematic diagram of the experiment. (A) Influence on CS thermal aggregation kinetics with increasing $E7_2$ ratios and (B) influence on CS thermal aggregation kinetics with increasing E7SOs ratios. The inset of panel B is the SDS−PAGE showing the soluble CS fraction obtained as described Materials and Methods. The E7SOs:CS molar ratio is indicated above each lane considering that each E7SOs oligomer is composed of 72 monomers as suggested by light scattering experiments (*19*). (C) Influence on firefly luciferase thermal aggregation kinetics with increasing $E7_2$ ratios and (D) influence on firefly luciferase thermal aggregation kinetics with increasing E7SOs ratios. For all graphs, aggregation in the presence of 0.9 μM BSA (□), no additive (○), 0.15 μM E7 (●), 0.45 μM E7 (■), and 0.9 μM E7 (▲). When luciferase aggregation curves were recorded in the presence of $E7_2$ (C), the final scattering signal was higher than in the presence of BSA or without any additive, probably due to the aggregate size, indicating the different morphology of the luciferase aggregate or the co-aggregation of $E7_2$ with luciferase. Both CS and firefly luciferase were added after the baseline signal was recorded for 150 s to a final concentration of 0.15 μM; the arrow indicates addition of the protein. Thermal aggregation of CS was followed by recording light scattering at 360 nm in a Jasco V-550 spectrophotometer, and thermal aggregation of firefly luciferase was followed by recording light scattering at 360 nm in an Aminco Bowman spectrofluorimeter.

Another way to test for chaperone activity is by measuring its ability to prevent the spontaneous aggregation that takes place upon dilution of chemically unfolded CS into a folding buffer. When chemically unfolded CS was diluted into zero denaturant buffer in the absence of additives, the protein slowly aggregated (Figure 2A). Addition of $E7_2$ does not prevent this aggregation, but E7SOs almost entirely suppress it (Figure 2B). Addition of a 6-fold molar excess of BSA or chymotrypsin inhibitor-2 (not shown) failed to prevent thermal or chemical denaturant-mediated aggregations. Ad-

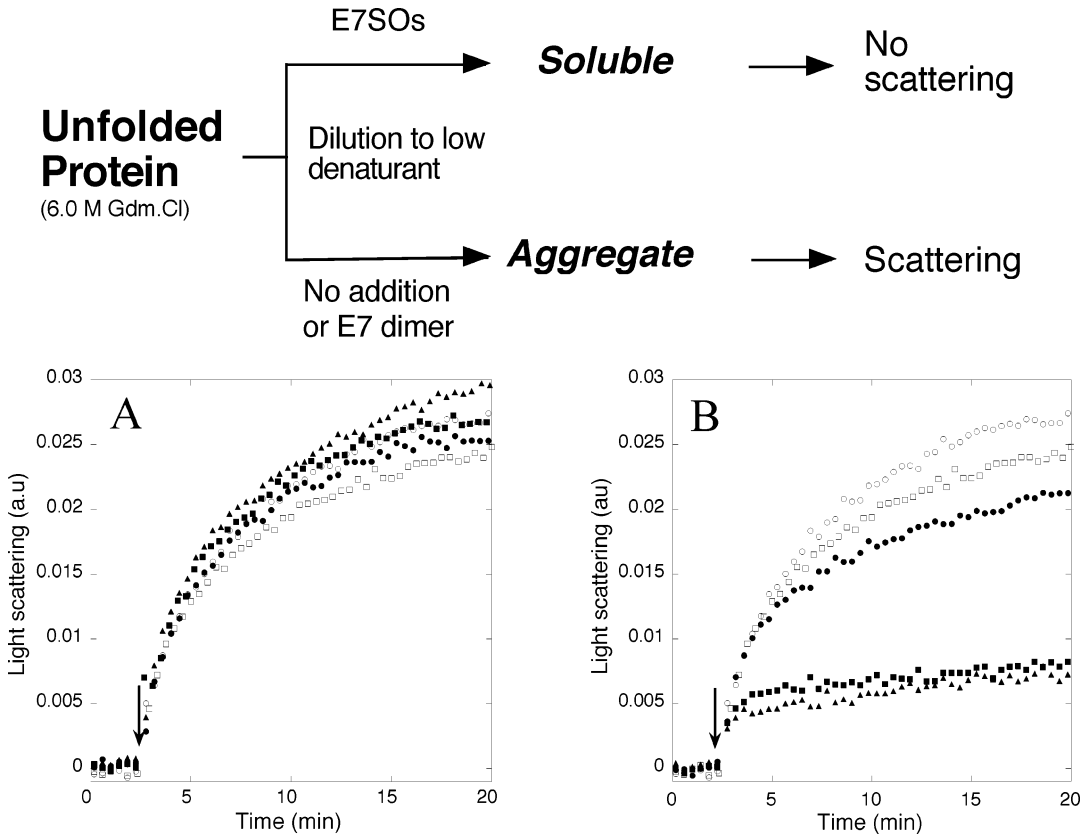

FIGURE 2: Chaperone activity of E7SOs chemically unfolded CS. The top panel is a schematic diagram of the experiment. (A) Aggregation kinetics of chemically unfolded CS with increasing ratios of $E7_2$ and (B) aggregation kinetics of chemically unfolded CS with increasing ratios of E7SOs. For both graphs, aggregation in the presence of 0.9 μM BSA (□), no additive (○), 0.15 μM E7 (●), 0.45 μM E7 (■), and 0.9 μM E7 (▲). Chemically unfolded CS was diluted in refolding buffer (see Materials and Methods) after the baseline signal was recorded for 150 s to a final concentration of 0.15 μM. The arrow indicates the addition of the protein. Aggregation occurs to some extent during the mixing time, independent of the E7 concentration probably due to the difference in kinetics between self-aggregation and E7SOs−CS interaction.

dition of a 6-fold molar excess of the N-terminal domain of E7, E7(1−40), containing the LXCXE motif, does not yield chaperone activity (not shown).

E7SOs Stably Bind the Model Polypeptide Substrates. To define the type of chaperone activity that E7SOs exert, we asked ourselves whether the suppression of the aggregation can be due to a transient interaction of E7SOs with the polypeptide substrate. Alternatively, they could form stable complexes in which the polypeptide remains bound even after cooling the sample to 25 °C. We next analyzed the interaction using size exclusion chromatography. After E7SOs and native dimeric CS were incubated together at 25 °C, no interaction was observed and each protein ran as a single separate peak, corresponding to E7SOs (790 kDa) and CS (98 kDa). This was confirmed by SDS−PAGE analysis of each peak (Figure 3 and its inset). No interaction was, therefore, observed for the folded substrate protein and the E7 chaperone.

When CS was heated to 45 °C in the presence of E7SOs as in the chaperone assay (Figure 1B), incubated for 30 min, and cooled slowly to 25 °C, a peak appeared in the exclusion volume of the column (BioSil 400, ∼1 MDa) corresponding to a complex between E7SOs and CS, with a concomitant decrease in the level of the individual species, as the silver-stained PAGE indicates (Figure 3 and its inset). As a control, we injected isolated E7SOs after heating, and no changes in the shape of the chromatogram were observed (not shown), which is in good agreement with the fact that

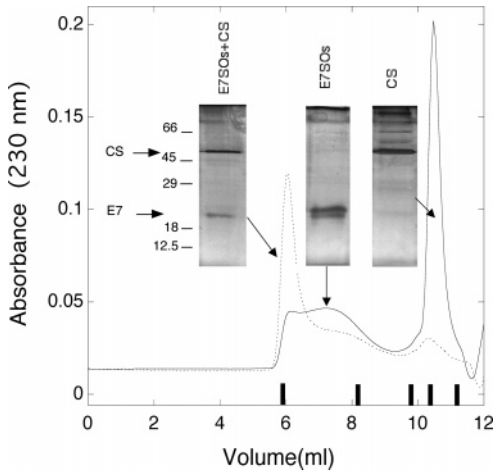

FIGURE 3: Formation of a stable E7SOs−substrate complex. Size exclusion chromatography of the CS−E7SOs complex was carried out as described in Materials and Methods: CS and E7SOs incubated at 25 °C (—) and CS and E7SOs incubated at 45 °C (•••). Bars denote molecular mass standards, from left to right: void volume and 670, 158, 44, and 17 kDa (Bio-Rad standards). The insets show silver-stained SDS−PAGE gels of TCA-precipitated protein fractions corresponding to each peak.

no substantial conformational changes were observed when the E7SOs sample was heated even at temperatures as high as 80 °C (*19*). CS or luciferase heated alone quickly aggregates, and after centrifugation, no sample is left for analysis and no peaks are observed by size exclusion

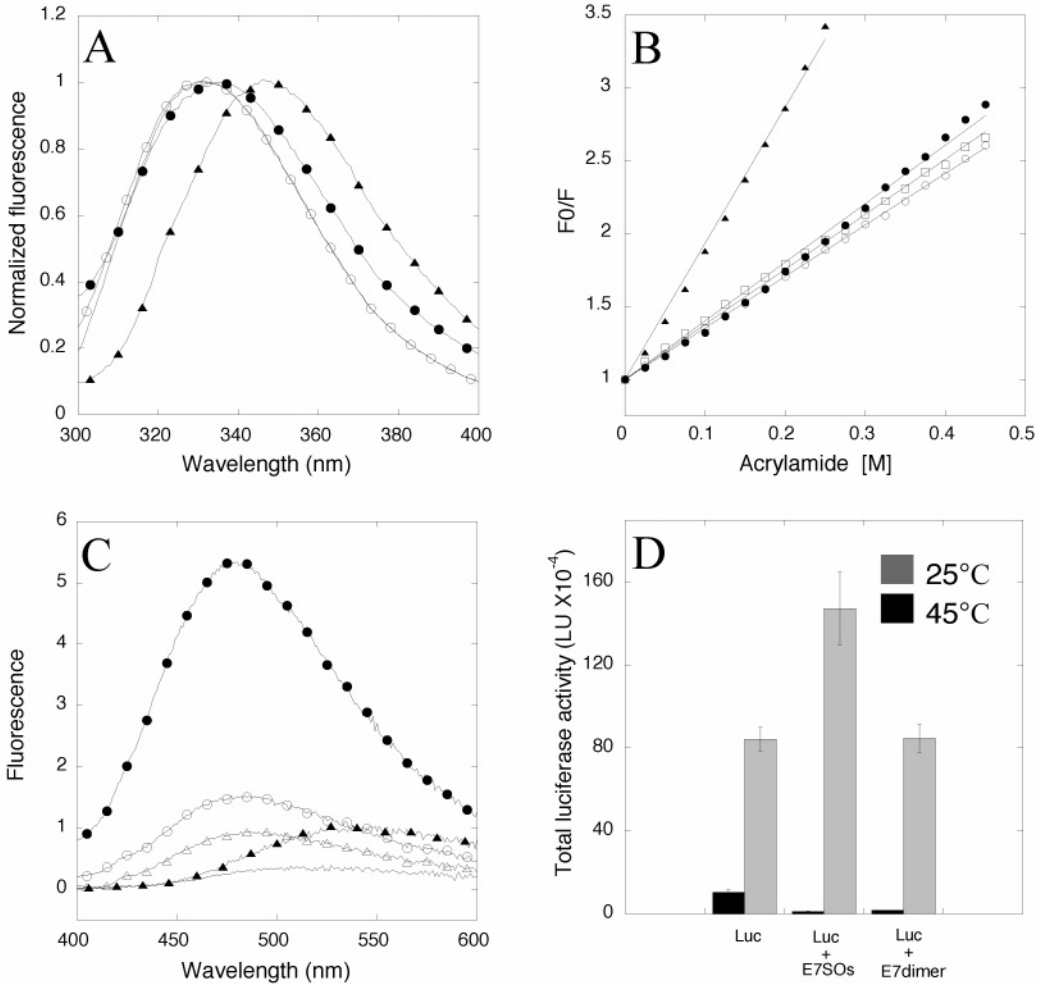

FIGURE 4: Conformational state of E7SOs-bound substrates. (A) Normalized tryptophan emission fluorescence of CS bound to E7SOs: CS incubated at 25 °C (—), CS and E7SOs incubated at 25 °C (○), CS and E7SOs incubated at 45 °C (●), and CS in 6.0 M Gdm·Cl (▲). (B) Quenching of CS bound to E7SOs by acrylamide: CS at 25 °C (□), CS and E7SOs incubated at 25 °C (○), CS and E7SOs incubated at 45 °C (●), and CS in 6 M Gdm·Cl (▲). (C) ANS fluorescence of CS bound to E7SOs: CS at 25 °C (—), CS and E7SOs incubated at 25 °C (○), CS and E7SOs incubated at 45 °C (●), E7SOs incubated at 45 °C (△), and CS in 6.0 M Gdm·Cl (▲). (D) Luciferase activity of the complex. An average of three measurements at 25 or 45 °C was plotted for each sample.

chromatography (SEC). Similarly, E7SOs form stable complexes with luciferase (not shown). These data are consistent with a "chaperone holdase" activity of E7SOs; i.e., they can prevent protein aggregation by binding and keeping the substrate protein in a stable complex.

Substrate Proteins Are Bound to the E7 Chaperone in a Structured State. HPV-16 E7 protein has no tryptophan (Trp) residues in its sequence, which facilitates the conformational study of the bound proteins by using the intrinsic Trp fluorescence of the polypeptide substrate (*27*, *28*). Trp emission spectra strongly depend on the polarity of the environment, and thus on the solvent accessibility of the site. The fluorescence emission maximum is shifted to longer wavelengths as a protein unfolds partially or completely, since its Trp residues become accessible to the aqueous solvent. We treated CS, containing nine Trp residues, at 45 °C in the presence of E7SOs to form the chaperone−substrate complex, and we cooled the solution to 25 °C and analyzed its fluorescence spectrum (same conditions as in Figure 3). Figure 4A shows that the normalized fluorescence emission spectrum of CS bound to E7SOs (λ_{max} = 331 nm; Table 1) is almost identical to that of CS alone or in the presence of E7SOs incubated at 25 °C, consistent with the Trp residues remaining less accessible to the solvent. As expected, it differs substantially from that of the chemically unfolded CS in guanidine hydrochloride (Gdm·Cl) with a red shift of 16 nm, consistent with the chromophores being fully accessible to the solvent (Table 1). Similar results were obtained with luciferase spectra which contain only one Trp residue ($\lambda_{max} \sim$ 330 nm, Table 1) with a red shift in its maximum emission wavelength of 18 nm when the protein is chemically unfolded, and with no significant shift when the luciferase sample is incubated with E7SOs at 25 or 45 °C.

Table 1: Characterization of the E7SOs-Bound Substrate Proteins

	temp (°C)	λ_{max} (nm)	K_q (M^{-1})	ANS (arbitrary units)	activity ($\times 10^{-4}$ arbitrary units)
CS	25	332	3.8	0.3	nd[a]
CS and E7SOs	25	331	3.5	1.5	nd[a]
CS and E7SOs	45	334	4.0	5.4	nd[a]
CS and Gdm·Cl	25	348	10.3	0.6	nd[a]
Luc	25	330	nd[a]	1.7	84
Luc and E7SOs	25	330	nd[a]	1.7	146
Luc and E7SOs	45	329	nd[a]	4.6	1.2
Luc and Gdm·Cl	25	348	nd[a]	0.1	nd[a]

[a] Not determined.

Acrylamide quenching of Trp residues in proteins provides a direct measurement of the solvent accessibility of the chromophore, and we used this approach as an additional and highly sensitive probe for the conformational state of the bound polypeptide substrate. The data of the fluorescence quenching of CS versus acrylamide concentration are linear, and the apparent quenching constants, K_q, are obtained from the Stern−Volmer plots (Figure 4B and Table 1). While Gdm·Cl-unfolded CS shows the highest accessibility (K_q = 10.3 M^{-1}), folded CS alone, CS with E7SOs incubated at 25 °C, and the CS−E7SOs complex formed by incubation at 45 °C show identical values within experimental error. On the basis of the environment of the Trp residues as sensitive probes, there is a substantial amount of tertiary structure. However, the native CS protein does not bind to the E7 chaperone at 25 °C (Figure 3).

What is the difference between the full native protein substrate that does not bind the chaperone holdase and the bound structure that was at least partially denatured by heat treatment? Two additional approaches were used to address this question. The first was an ANS binding experiment, since this dye is known to bind solvent accessible hydrophobic but otherwise structured patches in conformations close to the native state or non-native such as molten globules (*29*). As expected from the absence of tertiary or secondary structure in the chemically unfolded CS, this species does not bind ANS significantly, nor does the compact native CS (Figure 4C). The mixture of E7SOs and CS at 25 °C exhibited weak ANS binding, corresponding to the sum of the ANS binding of each molecule, and the same is observed for E7SOs incubated alone at 45 °C as a control, which were previously shown to bind ANS (*19*). The E7SOs−CS complex shows a 4-fold increase in the level of ANS binding with respect to the basal level of ANS binding of the noninteracting molecules (Figure 4C and Table 1). The same analysis was performed with luciferase, and similar results were obtained (Table 1).

The second approach to finely discriminate between the free folded protein and the chaperone bound near-native protein is enzymatic activity. Luciferase is a good substrate for chaperone studies because of a highly specific and sensitive activity that can be measured easily in the context of a mixture of proteins and various conditions. Luciferase activity dramatically decreases after the protein is heated at 45 °C, but unlike the conformational effect detected with spectroscopic probes, the addition of the E7SO chaperone does not prevent the decrease in enzymatic activity (Figure 4D and Table 1). The lack of activity for the heated luciferase alone or with $E7_2$ is due to sample loss upon aggregation, as the sample is centrifuged before activity measurements. However, luciferase heated in the presence of E7SOs remains in the solution, indicating that the decrease in activity is not due to aggregation-mediated sample loss. Therefore, the lack of activity recovery clearly indicates that the protein is not fully native when bound to the chaperone. The complex formed by luciferase and E7SOs cannot be dissociated by cooling the solution to 25 °C.

The N-Terminal Domain of E7 Is Exposed to the Solution in the E7SOs. There is no structural information for any of the E7 forms, and we addressed the topology of the N-terminal domain on the spherical assembly of E7SOs, since the minimal canonical Rb binding site

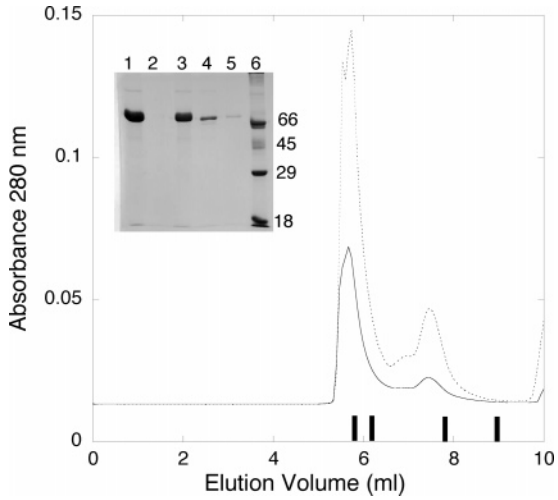

FIGURE 5: Topology of the N-terminus of E7SOs using a MBP−E7 fusion protein. Size exclusion chromatography of the MBP−E7SOs fusion protein obtained by treating the MBP−E7 dimer with EDTA (···) and MBP−E7SOs fusion protein recovered from amylose beads after elution with maltose (−). Bars denote molecular mass standards, from left to right: void volume (blue dextran) and 670, 158, and 44 kDa (Bio-Rad standards). The inset shows SDS−PAGE of MBP−E7 samples bound to amylose beads: lane 1, total protein; lane 2, amylose beads; lane 3, MBP−E7SOs fusion protein bound to amylose beads; lane 4, MBP−E7SOs fusion protein eluted from amylose beads with 15 mM maltose; lane 5, amylose beads after elution with a maltose solution; and lane 6, molecular mass markers (kilodaltons).

(LXCXE) spans residues 22−26 and has to be fully accessible to the target protein for interaction. In addition, it would provide clues for identifying the domain of E7 responsible for binding to the polypeptide substrates. To address this, we analyzed the ability of a maltose binding protein−E7 (MBP−E7) fusion protein to form oligomers. Addition of EDTA causes the fusion protein to assemble into large oligomers in a manner similar to that of nonfused E7, as the species eluting in the exclusion volume of the SEC experiment indicates (Figure 5). However, the location of the large MBP tag protein (∼45 kDa) in this structure is not easily predicted. We carried out amylose binding experiments (the specific ligand for MPB is maltose) in which the MBP−E7SOs fusion protein was incubated with amylose resin, centrifuged, and analyzed by SDS−PAGE to assess whether these oligomers can bind amylose, as expected if MBP was located facing the outer side of the spherical assembly. MBP−E7SOs fusion protein can bind to the amylose resin (Figure 5, inset, lane 3), and this binding is displaced by maltose (Figure 5, inset, lane 4), indicating that the interaction is specific. The species recovered from the amylose resin was confirmed to be MBP−E7SOs fusion protein in a SEC experiment (Figure 5, solid line). As the C-terminal Zn binding domain is thought to be responsible for the oligomerization properties of the E7 protein [i.e., dimerization (*17*, *30*, *31*)] and for the formation of E7SOs (*19*), these results fit well with a model in which the N-terminal domain is facing outward in the oligomeric assembly.

Rb Binding Properties of the E7 Chaperone. Papillomavirus E7 is closely related to the E1A protein from adenovirus and SV40 large T-antigen from polyomavirus in both sequence and biological function (*4*, *11*, *32*). The mechanisms by which these proteins act share some properties. They need

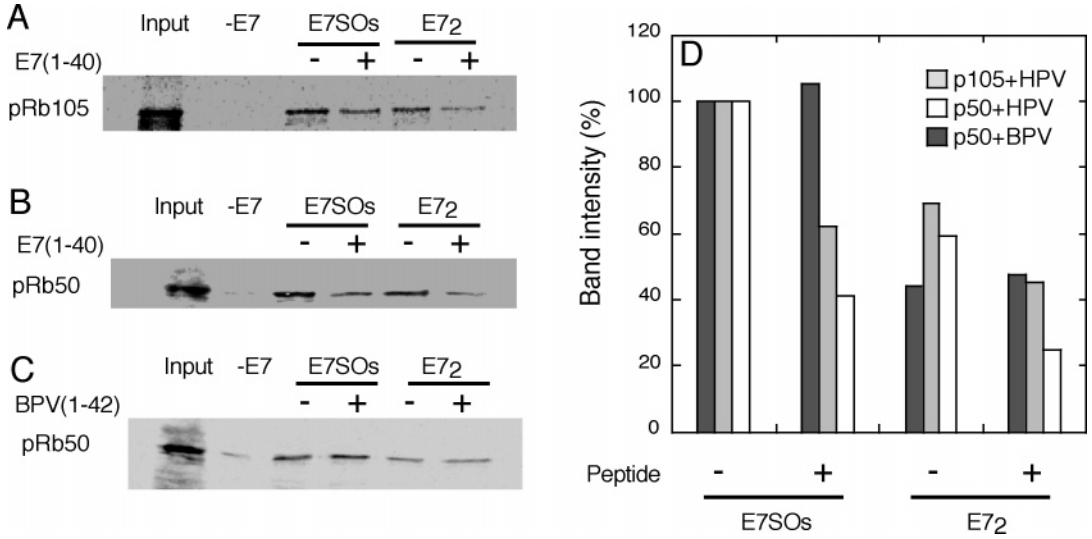

FIGURE 6: Rb binding of E7 species by immunoprecipitation. The experiments were performed using "in vitro" translated pRb105, and pRb50 under conditions described in Materials and Methods. (A) E7SOs and $E7_2$ bind full-length pRb105, and this interaction can be partially offset by the E7(1−40) peptide. (B) Both E7 species bind a truncated form of retinoblastoma protein, pRb50, and this interaction can be partially offset by the E7(1−40) peptide. (C) The binding of E7SOs and $E7_2$ to pRb 50 cannot be offset by the N-terminal domain of E7 BPV1 that lacks the canonical pRb-binding motif. (D) Band intensities of the experiments shown in panels A−C were analyzed quantitatively. The intensity of each band was normalized to the intensity of the E7SOs-bound pRb. In all cases, the intensity of the band corresponding to the $E7_2$-bound pRb was less intense. Considering the input band intensity, the amount of pRb bound to E7 in all the experiments ranged between 20 and 40% of the total and was independent of the E7 concentration added (not shown), indicating that some pRb population exists in a noncompetent binding conformation. For competition experiments, the peptide was added to a final concentration of 100 μM.

at least two independent nonoverlapping pRb binding sites to effectively disrupt the pRb−E2F complex (*25*, *33*, *34*). The SV40 large T-antigen shows an indirect mechanism in which the chaperone activity of its J-domain is strictly necessary to activate the host Hsp70 chaperone, which is in turn responsible for the release of E2F from pRb (*25*, *35*). It has been shown that binding of HPV-16 E7 to pRb at the CR2 domain alone is not sufficient to cause the release of the active form of E2F; it needs to interact with a second independent binding site located between residues 50 and 75 of HPV-16 E7 (*36*).

With this in mind, we aimed to evaluate the binding of both E7SOs and $E7_2$ species to the pRb protein, p105, which contains the minimal E7 binding domain (AB pocket) and the C-terminal domain responsible for E2F binding and the low-affinity E7 binding site (*36*). Two forms of pRb, p105 and p50 (AB pocket), were in vitro translated, challenged with the two E7 species, immunoprecipitated with an anti-E7 monoclonal antibody, and analyzed via SDS−PAGE. Both $E7_2$ and E7SOs bind p105 and p50 (Figure 6A,B), and the ∼50% increase in radioactivity suggests a tighter binding for the chaperone. If we consider the higher molecularity of E7SOS, this binding is effectively much tighter in molar terms. Both complexes of pRb and E7 can be displaced by the N-terminal domain of E7 [E7(1−40)] containing the LXCXE pRb binding motif (Figure 6A,B). Quantitative analysis shows that E7(1−40) displaces the respective complexes by 50% (Figure 6D). When the N-terminal domain of BPV-1 E7 which does not contain the canonical pRb binding site (LSPCAG instead of LXCXE) was used as the competitor peptide under identical conditions, no displacement of the pRb−E7 complex was observed (Figure 6C,D).

DISCUSSION

Information about the structure and biochemical mechanism of the E7 oncoprotein has been scarce so far, especially so if one considers the wealth of biological information, the number of targets it can bind, and the wide number of cellular pathways it is reported to affect, including its well-known ability to produce cellular transformation in arrested cells. From a conformational point of view, the increase in solvent accessibility to hydrophobic surfaces of $E7_2$ upon pH changes within the physiological range and at mild denaturant concentrations suggests conformational properties that could have evolved to enable protein−protein recognition of a large number of cellular binding partners (*18*). As previously shown, HPV-16 E7 can form high-molecular mass oligomers enriched in repetitive β-sheet structure (*19*) like those described for the small heat shock protein family sHSP (*37*), such as α crystallin (*21*) and HSP 16.5 (*38*). These HSPs act as chaperone holdases without the requirement of ATP, binding to non-native substrates in a nonspecific manner while keeping the bound protein in a folding-competent state (*39*). As described in the Results, several lines of evidence led us to consider a possible chaperone activity in E7.

In this work, we show that the oligomeric form of E7, E7SOs, and not the dimer, can bind and prevent aggregation of nonviral proteins normally used as standard chaperone substrates. On the basis of the molecular mass of E7SOs, 790 kDa (*19*), we estimate around 70 E7 monomers per oligomer, which is supported by stoichiometric titration. However, geometric constraints could prevent accommodation of a large number of bound molecules. Nevertheless, MBP−E7 fusion protein can readily form oligomers with the MPB protein facing the solution, indicating that there is

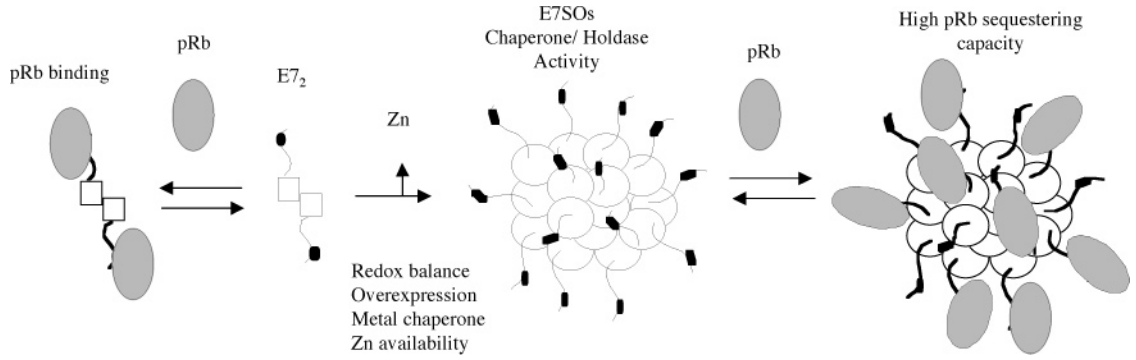

FIGURE 7: Minimal model for E7 conformers and pRb complexes in solution.

a particular radial arrangement such that the oligomerization tolerates the presence of a rather bulky protein such as MBP.

Folded substrate polypeptides do not bind to the chaperone at all; instead, they have to be in the process of either folding or unfolding, as chemical and thermal denaturation experiments showed. Both polypeptide substrates remain strongly bound to the E7 chaperone, and their conformation is spectroscopically similar to the compact native state, except for the lack of enzymatic activity in the case of luciferase. Thus, the E7 chaperone could bind late intermediates in the folding pathway or only partly unfolded polypeptides, arising from the relatively mild heat treatment. This property could allow E7SOs to sense small conformational perturbations on target proteins arising from constitutive or inducible regulatory post-translational modifications such as phosphorylation. The low binding specificity of chaperone activity may account for the wide range of cellular targets reported for E7 (*1*, *6*). However, it is unlikely that the chaperone activity of E7 is involved in general cellular protein folding pathways, mainly because the low cellular levels of E7 would not allow stoichiometrical reactions. Nevertheless, there are other processes in which chaperone activity is necessary, such as the disruption of protein−protein complexes and the degradation of cellular targets through the proteasome pathway (*40*, *41*), processes in which HPV-16 E7 has been shown to be involved (*14*, *42*).

Transforming proteins from DNA tumor viruses, namely, SV40 large T-antigen, adenovirus E1A, E7 from HPV, and, more recently, Tax protein from HTLV-1 (*43*), require two independent regions to disrupt pRb−E2F complexes (*44*). A high-affinity site including the canonical LXCXE sequence binds to the pRb AB pocket, but the isolated N-terminal domain of E7 containing the LXCXE is unable to release free active E2F; this feature is common to all these viral oncoproteins (*33*, *34*, *36*). A secondary site, located in different regions in each of the oncoproteins, is required for E2F dissociation, and a two-step hierarchical mechanism has been proposed. In HPV-16 E7, this site maps to the C-terminal domain, and this region should be exposed when the Zn atom is released. Although the mechanisms by which these proteins disrupt pRb−E2F complexes are similar, the SV40 large T-antigen does so indirectly by interacting through its J-domain with the cellular chaperone protein hsc70, a member of the hsp70 family (*35*). The chaperone activity of hsc70 is required for the inactivation of the pRb protein; moreover, the C-terminal domain of E7 is necessary for both pRb inactivation and h-Tid binding (*45*). The chaperone activity of E7 reported here could explain why the heterologous coexpression of the J-domain of the Hsj1 protein with HPV-16 E7 blocked the transactivation of E2F promoters in NIH3T3 cells (*25*). In addition, the human homologue of Hsj1, h-Tid, was shown to interact with the CR3 domain of E7, suggesting that a chaperone activity was involved in some way in the transforming activity of E7.

We analyzed the capacity of the two species of E7, dimer and chaperone oligomer, to bind to the pRb tumor suppressor. Both species bound the full-length pRb (p105) and p50 that includes the AB pocket domain, the primary interacting site (*46*). At 25 °C, the E7SOs appear to bind tighter than the dimer on a mass basis, and this difference is noticeable if one considers the higher stoichiometry and thus molecular avidity in the E7SOs. As opposed to its effect on the chaperone activity of E7, the E7(1−40) fragment is able to at least partially compete for pRb binding. This indicates that the basal pRb binding of E7SOs is separable from its chaperone activity on model substrates, in line with the presence of the high-affinity LXCXE pRb site in E7(1−40), which otherwise lacks chaperone activity. The absence of the C-terminal low-affinity binding site in pRb AB (p50) does not affect E7 binding.

Small perturbations of local or global stability in pRb can determine its potential recognition by the chaperone activity of E7. These perturbations may be temperature, other proteins, or post-translational modifications, acting as regulatory switches. This suggests two modes of action in antagonizing hypophosphorylated pRb. One would be binding of folded and/or stable species that would be active in sequestering E2F species but not directly involved in pRb degradation. However, as previously shown, the E7 binding site of pRb is located in the B domain but requires the A domain for stable binding of E7 (*46*, *47*); this strongly suggests that pRb is already marginally stable under conditions in which the model polypeptide substrates or other possible targets in vivo are stable. Therefore, specific binding would operate on pRb under basal conditions, while "less specific" and yet more avid binding would operate on both pRb and many of the reported targets.

The E7 chaperone activity on pRb or other targets could be involved in proteasome degradation, either dependent on or independent of ubiquitination. There is evidence that pRb degradation can be ubiquitin-independent, and the reported direct interaction of E7 with the S4 subunit of the 26S proteasome (*48*) suggests the latter route as being possible. Recent work demonstrated that ubiquitination alone is not enough for targeting a protein to the proteasome machinery to efficiently degrade it; an engaging signal is necessary,

and this second requirement is the availability of a partially unfolded region within the protein structure that could arise from a wrongly folded protein trapped by chaperone proteins or by an active unfolding process performed by chaperone unfoldase activities associated with the proteasome system (*40*). Additional local structural perturbations may well arise from modifications in temperature, redox state, and interaction with proteins, or post-translational modifications.

As recently proposed, both pRb antagonizing mechanisms of E7 and other LXCXE viral oncoproteins, i.e., sequestering pRb from E2F complexes and targeted destruction of pRb, need not be mutually exclusive, and binding of pocket proteins could be a step prior to degradation (*44*). Nevertheless, there is strong evidence that targeted degradation could be the bottleneck (*14*, *44*). E7 CR1 should therefore not be required for recruitment of cellular chaperones, since we now show that E7SOs exhibit a strong chaperone activity. Although the presence of the E7SOs is yet to be demonstrated in naturally infected cells, there is no indication so far about the E7 species that are populated in the cells. Given that E7 has a strongly conserved zinc binding motif and that it exhibits unusual conformational properties in solution, it is reasonable to assume that the zinc atom may have a regulatory role. Removal of the zinc atom readily yields E7SOs, and the apo-E7 monomeric or dimeric species is not populated at all. In addition, the E7SOs are thermodynamically more stable than $E7_2$, and the process is quasi-irreversible (*19*). Any physiological or stress situation that combines oxidation, a decrease in the level of zinc, and overexpression of E7 could give way to such oligomeric species. In any case, the conformational state of E7 in cells has not been established. A minimal model for the biochemical mechanism presented in this work is shown in Figure 7.

Although they share many properties, each of the known and new viral pRb targeting oncoproteins presents rather different domain arrangements, and they are multifunctional (*49*). The variability in their differential targeting and effects on cell cycle will contribute to the unraveling of the full mechanistic features of these lethal weapons. Structural and biochemical studies of the isolated oncoproteins and their targets will provide essential insight into their mechanisms of action and the most effective ways of controlling them.

ACKNOWLEDGMENT

We thank Eduardo Castaño and Julio Caramelo for criticism of the manuscript.

REFERENCES

1. Munger, K. (2002) The role of human papillomaviruses in human cancers, *Front. Biosci. 7*, d641−9.
2. Tommasino, M., and Crawford, L. (1995) Human papillomavirus E6 and E7: Proteins which deregulate the cell cycle, *BioEssays 17*, 509−18.
3. Sato, H., Furuno, A., and Yoshiike, K. (1989) Expression of human papillomavirus type 16 E7 gene induces DNA synthesis of rat 3Y1 cells, *Virology 168*, 195−9.
4. Phelps, W. C., Yee, C. L., Munger, K., and Howley, P. M. (1988) The human papillomavirus type 16 E7 gene encodes transactivation and transformation functions similar to those of adenovirus E1A, *Cell 53*, 539−47.
5. Munger, K., and Phelps, W. C. (1993) The human papillomavirus E7 protein as a transforming and transactivating factor, *Biochim. Biophys. Acta 1155*, 111−23.
6. Munger, K., Basile, J. R., Duensing, S., Eichten, A., Gonzalez, S. L., Grace, M., and Zacny, V. L. (2001) Biological activities and molecular targets of the human papillomavirus E7 oncoprotein, *Oncogene 20*, 7888−98.
7. Munger, K., and Howley, P. M. (2002) Human papillomavirus immortalization and transformation functions, *Virus Res. 89*, 213−28.
8. Dyson, N., Howley, P. M., Munger, K., and Harlow, E. (1989) The human papilloma virus-16 E7 oncoprotein is able to bind to the retinoblastoma gene product, *Science 243*, 934−7.
9. Reinstein, E., Scheffner, M., Oren, M., Ciechanover, A., and Schwartz, A. (2000) Degradation of the E7 human papillomavirus oncoprotein by the ubiquitin-proteasome system: Targeting via ubiquitination of the N-terminal residue, *Oncogene 19*, 5944−50.
10. Oh, K. J., Kalinina, A., Wang, J., Nakayama, K., Nakayama, K. I., and Bagchi, S. (2004) The papillomavirus E7 oncoprotein is ubiquitinated by UbcH7 and Cullin 1- and Skp2-containing E3 ligase, *J. Virol. 78*, 5338−46.
11. Chellappan, S., Kraus, V. B., Kroger, B., Munger, K., Howley, P. M., Phelps, W. C., and Nevins, J. R. (1992) Adenovirus E1A, simian virus 40 tumor antigen, and human papillomavirus E7 protein share the capacity to disrupt the interaction between transcription factor E2F and the retinoblastoma gene product, *Proc. Natl. Acad. Sci. U.S.A. 89*, 4549−53.
12. Jones, D. L., Thompson, D. A., and Munger, K. (1997) Destabilization of the RB tumor suppressor protein and stabilization of p53 contribute to HPV type 16 E7-induced apoptosis, *Virology 239*, 97−107.
13. Wang, J., Sampath, A., Raychaudhuri, P., and Bagchi, S. (2001) Both Rb and E7 are regulated by the ubiquitin proteasome pathway in HPV-containing cervical tumor cells, *Oncogene 20*, 4740−9.
14. Gonzalez, S. L., Stremlau, M., He, X., Basile, J. R., and Munger, K. (2001) Degradation of the retinoblastoma tumor suppressor by the human papillomavirus type 16 E7 oncoprotein is important for functional inactivation and is separable from proteasomal degradation of E7, *J. Virol. 75*, 7583−91.
15. Fiedler, M., Muller-Holzner, E., Viertler, H. P., Widschwendter, A., Laich, A., Pfister, G., Spoden, G. A., Jansen-Durr, P., and Zwerschke, W. (2004) High level HPV-16 E7 oncoprotein expression correlates with reduced pRb-levels in cervical biopsies, *FASEB J. 18*, 1120−2.
16. Heck, D. V., Yee, C. L., Howley, P. M., and Munger, K. (1992) Efficiency of binding the retinoblastoma protein correlates with the transforming capacity of the E7 oncoproteins of the human papillomaviruses, *Proc. Natl. Acad. Sci. U.S.A. 89*, 4442−6.
17. McIntyre, M. C., Frattini, M. G., Grossman, S. R., and Laimins, L. A. (1993) Human papillomavirus type 18 E7 protein requires intact Cys-X-X-Cys motifs for zinc binding, dimerization, and transformation but not for Rb binding, *J. Virol. 67*, 3142−50.
18. Alonso, L. G., Garcia-Alai, M. M., Nadra, A. D., Lapena, A. N., Almeida, F. L., Gualfetti, P., and Prat-Gay, G. D. (2002) High-risk (HPV16) human papillomavirus E7 oncoprotein is highly stable and extended, with conformational transitions that could explain its multiple cellular binding partners, *Biochemistry 41*, 10510−8.
19. Alonso, L. G., Garcia-Alai, M. M., Smal, C., Centeno, J. M., Iacono, R., Castano, E., Gualfetti, P., and de Prat-Gay, G. (2004) The HPV16 E7 viral oncoprotein self-assembles into defined spherical oligomers, *Biochemistry 43*, 3310−7.
20. Smotkin, D., and Wettstein, F. O. (1987) The major human papillomavirus protein in cervical cancers is a cytoplasmic phosphoprotein, *J. Virol. 61*, 1686−9.
21. Horwitz, J. (1992) α-Crystallin can function as a molecular chaperone, *Proc. Natl. Acad. Sci. U.S.A. 89*, 10449−53.
22. Ehrnsperger, M., Graber, S., Gaestel, M., and Buchner, J. (1997) Binding of non-native protein to Hsp25 during heat shock creates a reservoir of folding intermediates for reactivation, *EMBO J. 16*, 221−9.
23. Haley, D. A., Bova, M. P., Huang, Q. L., McHaourab, H. S., and Stewart, P. L. (2000) Small heat-shock protein structures reveal a continuum from symmetric to variable assemblies, *J. Mol. Biol. 298*, 261−72.
24. Chang, Z., Primm, T. P., Jakana, J., Lee, I. H., Serysheva, I., Chiu, W., Gilbert, H. F., and Quiocho, F. A. (1996) *Mycobacterium tuberculosis* 16-kDa antigen (Hsp16.3) functions as an oligomeric structure in vitro to suppress thermal aggregation, *J. Biol. Chem. 271*, 7218−23.
25. Sheng, Q., Denis, D., Ratnofsky, M., Roberts, T. M., DeCaprio, J. A., and Schaffhausen, B. (1997) The DnaJ domain of polyo-

mavirus large T antigen is required to regulate Rb family tumor suppressor function, *J. Virol. 71*, 9410−6.
26. Buchner, J., Grallert, H., and Jakob, U. (1998) Analysis of chaperone function using citrate synthase as nonnative substrate protein, *Methods Enzymol. 290*, 323−38.
27. Das, K. P., Petrash, J. M., and Surewicz, W. K. (1996) Conformational properties of substrate proteins bound to a molecular chaperone α-crystallin, *J. Biol. Chem. 271*, 10449−52.
28. Mendoza, J. A., Butler, M. C., and Horowitz, P. M. (1992) Characterization of a stable, reactivatable complex between chaperonin 60 and mitochondrial rhodanese, *J. Biol. Chem. 267*, 24648−54.
29. Kirk, W. R., Kurian, E., and Prendergast, F. G. (1996) Characterization of the sources of protein−ligand affinity: 1-Sulfonato-8(1′)-anilinonaphthalene binding to intestinal fatty acid binding protein, *Biophys. J. 70*, 69−83.
30. Clemens, K. E., Brent, R., Gyuris, J., and Munger, K. (1995) Dimerization of the human papillomavirus E7 oncoprotein in vivo, *Virology 214*, 289−93.
31. Clements, A., Johnston, K., Mazzarelli, J. M., Ricciardi, R. P., and Marmorstein, R. (2000) Oligomerization properties of the viral oncoproteins adenovirus E1A and human papillomavirus E7 and their complexes with the retinoblastoma protein, *Biochemistry 39*, 16033−45.
32. Barbosa, M. S., Edmonds, C., Fisher, C., Schiller, J. T., Lowy, D. R., and Vousden, K. H. (1990) The region of the HPV E7 oncoprotein homologous to adenovirus E1a and Sv40 large T antigen contains separate domains for Rb binding and casein kinase II phosphorylation, *EMBO J. 9*, 153−60.
33. Huang, P. S., Patrick, D. R., Edwards, G., Goodhart, P. J., Huber, H. E., Miles, L., Garsky, V. M., Oliff, A., and Heimbrook, D. C. (1993) Protein domains governing interactions between E2F, the retinoblastoma gene product, and human papillomavirus type 16 E7 protein, *Mol. Cell. Biol. 13*, 953−60.
34. Fattaey, A. R., Harlow, E., and Helin, K. (1993) Independent regions of adenovirus E1A are required for binding to and dissociation of E2F-protein complexes, *Mol. Cell. Biol. 13*, 7267−77.
35. Sullivan, C. S., Cantalupo, P., and Pipas, J. M. (2000) The molecular chaperone activity of simian virus 40 large T antigen is required to disrupt Rb-E2F family complexes by an ATP-dependent mechanism, *Mol. Cell. Biol. 20*, 6233−43.
36. Patrick, D. R., Oliff, A., and Heimbrook, D. C. (1994) Identification of a novel retinoblastoma gene product binding site on human papillomavirus type 16 E7 protein, *J. Biol. Chem. 269*, 6842−50.
37. Bova, M. P., Ding, L. L., Horwitz, J., and Fung, B. K. (1997) Subunit exchange of αA-crystallin, *J. Biol. Chem. 272*, 29511−7.
38. Kim, K. K., Kim, R., and Kim, S. H. (1998) Crystal structure of a small heat-shock protein, *Nature 394*, 595−9.
39. Lee, G. J., Roseman, A. M., Saibil, H. R., and Vierling, E. (1997) A small heat shock protein stably binds heat-denatured model substrates and can maintain a substrate in a folding-competent state, *EMBO J. 16*, 659−71.
40. Lee, C., Schwartz, M. P., Prakash, S., Iwakura, M., and Matouschek, A. (2001) ATP-dependent proteases degrade their substrates by processively unraveling them from the degradation signal, *Mol. Cell 7*, 627−37.
41. Braun, B. C., Glickman, M., Kraft, R., Dahlmann, B., Kloetzel, P. M., Finley, D., and Schmidt, M. (1999) The base of the proteasome regulatory particle exhibits chaperone-like activity, *Nat. Cell Biol. 1*, 221−6.
42. Banks, L., Pim, D., and Thomas, M. (2003) Viruses and the 26S proteasome: Hacking into destruction, *Trends Biochem. Sci. 28*, 452−9.
43. Kehn, K., Fuente Cde, L., Strouss, K., Berro, R., Jiang, H., Brady, J., Mahieux, R., Pumfery, A., Bottazzi, M. E., and Kashanchi, F. (2005) The HTLV-I Tax oncoprotein targets the retinoblastoma protein for proteasomal degradation, *Oncogene 24*, 525−40.
44. Helt, A. M., and Galloway, D. A. (2003) Mechanisms by which DNA tumor virus oncoproteins target the Rb family of pocket proteins, *Carcinogenesis 24*, 159−69.
45. Schilling, B., De-Medina, T., Syken, J., Vidal, M., and Munger, K. (1998) A novel human DnaJ protein, hTid-1, a homolog of the *Drosophila* tumor suppressor protein Tid56, can interact with the human papillomavirus type 16 E7 oncoprotein, *Virology 247*, 74−85.
46. Lee, J. O., Russo, A. A., and Pavletich, N. P. (1998) Structure of the retinoblastoma tumour-suppressor pocket domain bound to a peptide from HPV E7, *Nature 391*, 859−65.
47. Chow, K. N., and Dean, D. C. (1996) Domains A and B in the Rb pocket interact to form a transcriptional repressor motif, *Mol. Cell. Biol. 16*, 4862−8.
48. Berezutskaya, E., and Bagchi, S. (1997) The human papillomavirus E7 oncoprotein functionally interacts with the S4 subunit of the 26S proteasome, *J. Biol. Chem. 272*, 30135−40.
49. Kalejta, R. F. (2004) Human cytomegalovirus pp71: A new viral tool to probe the mechanisms of cell cycle progression and oncogenesis controlled by the retinoblastoma family of tumor suppressors, *J. Cell. Biochem. 93*, 37−45.
50. Lakowicz, J. R. (1999) *Principles of Fluorescence Spectroscopy*, 2nd ed., Kluwer Academic, New York.

BI0522549